

Covalent Immobilization of Glucose Oxidase onto Electro-synthesized Nanocomposite with PEDOT Derivative for Amperometric Glucose Biosensing

Peicong Zhou^{1,*}, Fan Li^{1,2}, Wenjie Dong², Kai Huang², Yueyao Chen², Chao Wei¹, Bai Ling², Mingfang Li²

¹ Department of Physics, Jiangxi Agricultural University, Jiangxi, 330045, China

² Institute of Functional Materials and Agricultural Applied Chemistry, Jiangxi Agricultural University, Nanchang 330045, PR China

*E-mail: itsdaily@126.com

Received: 6 March 2018 / Accepted: 9 April 2018 / Published: 10 May 2018

A highly sensitive and specific glucose (Glu) amperometric biosensor was successfully developed by the covalent immobilization of glucose oxidase (GOx) onto the electro-synthesized ionic liquid (ILs) modified poly(3,4-ethylenedioxythiophene) derivative poly(hydroxymethylated-3,4-ethylenedioxythiophene) (PEDOTM) nanocomposite based on multi-walled carbon nanotubes functionalized with carboxyl group (MWCNTs-COOH). A highly-stable and conducting PEDOTM was one-step electro-synthesized in water/ILs mixed system containing BmimPF₆ and MWCNTs-COOH, then GOx was covalently immobilized onto the biocompatible ILs modified PEDOTM-MWCNTs-COOH with high affinity, which was employed for amperometric biosensing of Glu in human urine, human and animal serum samples. IL/PEDOTM-MWCNTs-COOH displayed good electrochemical activity, excellent electrochemical stability and high conductivity. The fabricated GOx biosensor showed pronounced amperometric current toward Glu response in a wide linear range of $6.0 \times 10^{-8} \sim 2 \times 10^{-3}$ M with a high sensitivity of $89.5 \mu\text{A M}^{-1} \text{cm}^{-2}$, rapid response time within 10 s, low limit of detection of 0.015 μM , remarkable biocompatibility and bioaffinity, high sensing stability, excellent selectivity and practicality. Satisfactory results reveal that the ILs-PEDOTM-MWCNTs-COOH will provide a promising biosensing platform for the covalent immobilization of biomacromolecules and disease diagnostics via the detection of Glu in human and animal serum samples.

Keywords: Biosensor, glucose oxidase, Ionic liquid, Multi-walled carbon nanotube, Poly(3,4-ethylenedioxythiophene), glucose

1. INTRODUCTION

Glucose (Glu) is one of the most essential chemical substances in organism and the main energy source in species. Moreover, the abnormal blood Glu in organism can cause a lot of diseases such as high blood pressure, diabetes, cardiovascular disease, retinopathy, and nephropathy. Therefore, it is very urgent to develop a facile analytical tool for disease diagnostics via highly-sensitive and specific measurement of Glu in human and animal body. Glu biosensors are one of simple analytical methods for the measurement of Glu due to its advantages including high specificity, rapid response, good selectivity, low cost, etc, which are now used for food industry, biological medicine, biochemical industry [1-3]. Among all Glu biosensors, electrochemical methods are new alternatives for the Glu detection due to its superior features of simple and portable instruments, fast response, and low cost [4, 5]. Moreover, glucose oxidase (GOx) biosensors are one of the most studied Glu biosensors [1, 5]. Meanwhile, different materials have been employed to the construction of efficient GOx biosensors with the development of science and technology [4, 5]. Conducting polymers (CPs) [6] and nanomaterials like various kinds of carbon materials [7] or a variety of noble metals and metal oxides [8] have received widespread attention for electrochemical Glu biosensors.

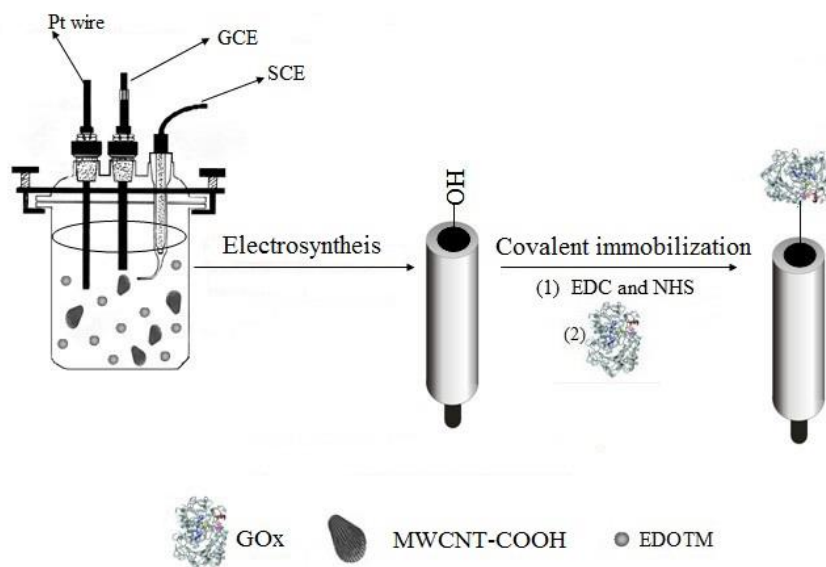
Poly (3, 4-ethylenedioxythiophene) (PEDOT) is one is outstanding CPs due to owing to its a high and stable conductivity, a relatively low bandgap and electro-oxidation potential, an excellent ability to be rapidly switched between conducting states and insulating states, a high degree of optical transparency as a conductor or semiconductor, easy electro-synthesis, and superior chemical stability and environmental stability [9-11]. Moreover, PEDOT possesses good biocompatibility, low toxicity and structural stability, great potential applications in the medical biosensing fields [11, 12]. However, the poor water solubility of 3,4-ethylenedioxythiophene (EDOT) is an important drawback, and one of methods are the addition of an appropriate pendant side group onto the backbone [11, 13]. Hydroxyl group functionalized EDOT (hydroxymethylated-3,4-ethylenedioxythiophene) (2,3-dihydrothieno[3,4-b][1,4]dioxin-2-yl) methanol (EDOTM) not only improved the solubility in water, but also enhanced biocompatibility. Therefore, this CPs was selected for applications in biology and related fields [14-17].

Ionic liquids (ILs) have environmentally benign features derived from the wide potential window, high-ionic conductivity, good electrochemical stability, high specific solvent ability and biocompatibility, which have been applied for stabilizing and activating enzymes [18] and electrochemical bio/chemo-sensors [19-22]. Moreover, the utility of ILs for the electrochemical preparation of CPs is very promising for electrochemical chemo/biosensors [23-25]. ILs/water system is an excellent, non-toxic, and cost-effective system for the electrochemistry of CPs by combing advantages of the two, and the electrosynthesis of PEDOT films in ILs/H₂O system indicated that ILs-in-water serves as the optimal system for the electro-polymerization of EDOT in comparison with water-in-ILs [26-28].

Carbon nanotubes(CNTs) have been widely employed for fabricating CNT-based electrochemical chemo/biosensors owing to their extraordinary electrochemical catalytic ability, excellent detectability, superior adsorption capacity, high active surface area, good conductivity, high chemical stability, readily modifiable surface, and satisfactory biocompatibility [29-33]. Carboxyl-

functionalized CNTs have obtained much concern in recent years owing to their ability to reinforce properties, enhance interfacial interactions, improve the solubility and covalent immobilization of biomacromolecules [29-31,34-37]. Moreover, there is a great many reports for CNT/PEDOT composites in electrochemical chemo/biosensors [36-41].

In this work, a highly stable and conducting PEDOTM-MWCNTs-COOH was electro-synthesized in water/ILs system containing BmimPF₆, then GOx was covalently immobilized onto biocompatible and conducting PEDOTM-MWCNTs-COOH (Scheme 1), which was employed for highly sensitive and specific amperometric biosensing of Glu in human and animal serum samples.



Scheme 1. The fabricated process of GCE/ILs-PEDOTM-MWCNTs-COOH/GOx for biosensing Glu.

2. EXPERIMENTALS

2.1 Materials

GOx (EC. 1.1.3.4) and 1-ethyl-3-(3-dimethylamio)propyl carbodiimide hydrochloride (EDC·HCl) were purchased from Aldrich. BmimPF₆ was obtained from Lanzhou Institute of Chemical Physics in Chinese Academy of Sciences. MWCNTs-COOH aqueous dispersion were purchased from Chengdu Institute of Organic Chemistry in Chinese Academy of Sciences. EDOTM was chemically synthesized according to previous reports [14,15]. Glu was bought from Guangzhou Chemical Reagent Factory. Disodium hydrogen phosphate dodecahydrate (Na₂HPO₄·12H₂O) and sodium dihydrogen phosphate dehydrate (NaH₂PO₄·2H₂O) were purchased from Sinopharm chemical reagent Co. Ltd. Phosphate buffer solution (PBS) was made from Na₂HPO₄ and NaH₂PO₄. N-Hydroxysuccinimide (NHS) was obtained from TCI. All chemicals were analytical grade and used without further purification. All solutions were prepared using deionized distilled water as solvent.

2.2 Apparatus

All electrochemical experiments were performed with a potentiostat–galvanostat (Model 263A, EG&G Princeton Applied Research) and CHI660E electrochemical workstation (Chenhua Instrument Co., Shanghai, China). The samples were added with the Finn pipette (Labsystems, Helsinki, Finland). The pH value was measured with a Delta 320 pH meter (Mettler-Toledo Instrument, Shanghai, China). The temperature was controlled with a type HHS thermostat (Shanghai, China). FT-IR Spectrometer were recorded using Bruker Vertex 70 Fourier transform infrared spectrometer with KBr pellets. The electrochemical impedance spectroscopy (EIS) were carried out in 5 mmol/L $[\text{Fe}(\text{CN})_6]^{3-/4-}$ containing 0.1 mol/L KCl at the open circuit potential with a frequency range from 0.01 Hz to 10^5 Hz and an amplitude of 5 mV.

2.3 Electrochemical Measurements

Electrochemical preparation and tests were performed in a one-compartment cell. a saturated calomel electrode (SCE) as the reference electrode, a working electrode was a glass carbon electrode (GCE) with a diameter of 3mm, and a platinum wire as the auxiliary electrode. All electrochemical measurements were carried out at room temperature. Prior to each measurement, the solution was stirred. GCE was polished with alumina ($\text{Al}_2\text{O}_3, 0.05 \mu\text{m}$), rinsed sequentially by ultrasonic cleaning in deionized water, ethanol and deionized water for 5 min and dried in air. The GCE/ILs-PEDOTM-MWCNTs-COOH/GOx was used as the working electrode. Each data point stands for the average of triplicate experiments.

2.4 Preparation of ILs-PEDOTM-MWCNTs-COOH

ILs-PEDOTM-MWCNTs-COOH was obtained by the one-step potentiostatical polymerization of 0.02 mol/L EDTM at 1.1 V vs SCE for 90 s in aqueous system containing BmimPF₆ (BmimPF₆/water with the volume ratio of 3:7) and 10 mM LiClO₄. The as-obtained ILs-PEDOTM-MWCNTs-COOH films were washed with deionized water to remove supporting electrolytes and adsorbed monomer from the surface of the working electrode.

2.5 Covalent Immobilization of GOx

After ILs-PEDOTM-MWCNTs-COOH films were electro-synthesized, then GOx were covalently immobilized. Initially, hydroxyl groups of PEDOTM and carboxylic groups of MWCNTs-COOH were activated by immersing in 50 mmol/L PBS (pH 7) containing 15 mmol/L EDC·HCl and 30 mmol/L NHS for 1.5 h, then immersed in PBS (pH 7) containing 0.3 mg mL^{-1} GOx at 4°C for 1.5 h to realize the covalent immobilization of GOx. During the above process, the covalent bond was formed between GOx and both PEDOTM and MWCNTs-COOH. The as-prepared biosensor based on

ILs-PEDOTM-MWCNTs-COOH/GOx was rinsed with PBS (pH 7) several times to remove free GOx and kept in PBS (pH 7) at 4°C when not in use.

2.6 Amperometric Detection of Glu

The amperometric detection of Glu was carried out in a standard solution at a working potential of 0.6V vs SCE. The different concentrations of Glu standard solution were prepared using 0.1M PBS (pH = 7). The fabricated ILs-PEDOTM-MWCNTs-COOH/GOx bioelectrode was served as the working electrode. All cells were set in a thermostat, in which the temperature can be set constant at 25°C.

2.7 Preparation of practical samples

All animal serums were obtained from the key laboratory of College of Animal Science and Technology in Jiangxi Agricultural University. Human urine and serum was obtained from healthy volunteers and collected by hospital in Jiangxi Agricultural University. All serums and urine were homogenized for 10 min, respectively. Then homogenates were filtered to remove residues. 0.1 M $\text{Na}_2\text{HPO}_4 \cdot 12\text{H}_2\text{O}$ and 0.1 M $\text{NaH}_2\text{PO}_4 \cdot 2\text{H}_2\text{O}$ were added into all obtained filtrates, respectively. Then the sample solutions (pH 7) were acquired. The GCE/ILs-PEDOTM-MWCNTs-COOH/GOx was applied for the measurements of all samples, then all samples were added into Glu with different concentrations using the standard addition method, respectively.

3. RESULTS AND DISCUSSION

3.1 Electrosynthesis of ILs-PEDOTM-MWCNTs-COOH

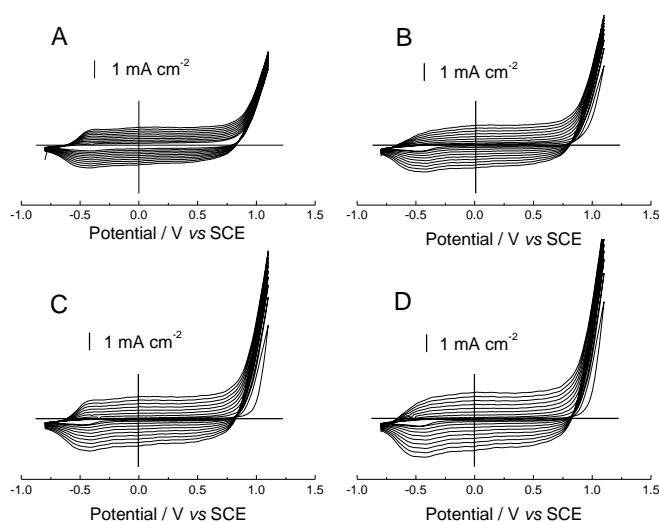


Figure 1. CVs of EDOTM in water/ILs mixed system containing BmimPF_6 and different mass of MWCNTs-COOH. No MWCNTs-COOH (A), and different mass ratios of MWCNTs-COOH to EDOTM (0.02 M) = 1:5 (B), 1:2 (C), 2:1 (D), respectively. Potential scan rates: 50 mV s^{-1} .

Fig. 1 shows successive cyclic voltammograms (CVs) of EDOTM in water containing BmimPF₆ and MWCNTs-COOH with different mass. All CVs exhibited similar CV characteristics (Fig. 1). The increasing redox currents with the increasing cycle number of potential scans implied that the ILs-PEDOTM-MWCNTs-COOH film was formed gradually onto the GCE surface. In addition, redox wave current densities of ILs-PEDOTM-MWCNTs-COOH obviously increased with the increasing MWCNTs-COOH content (Fig. 1B-D), indicating MWCNTs-COOH with good conductivity improved the conductivity of PEDOTM. Moreover, ILs as the charge-balancing dopant was very beneficial to the electrochemical polymerization of CPs, and CPs with higher conductivity could enhance the electron transfer for the application of chemo/bio sensors in electrochemistry [26-28].

3.2 Electrochemical properties of ILs-PEDOTM-MWCNTs-COOH

3.2.1 Electrochemical behaviors of ILs-PEDOTM-MWCNTs-COOH

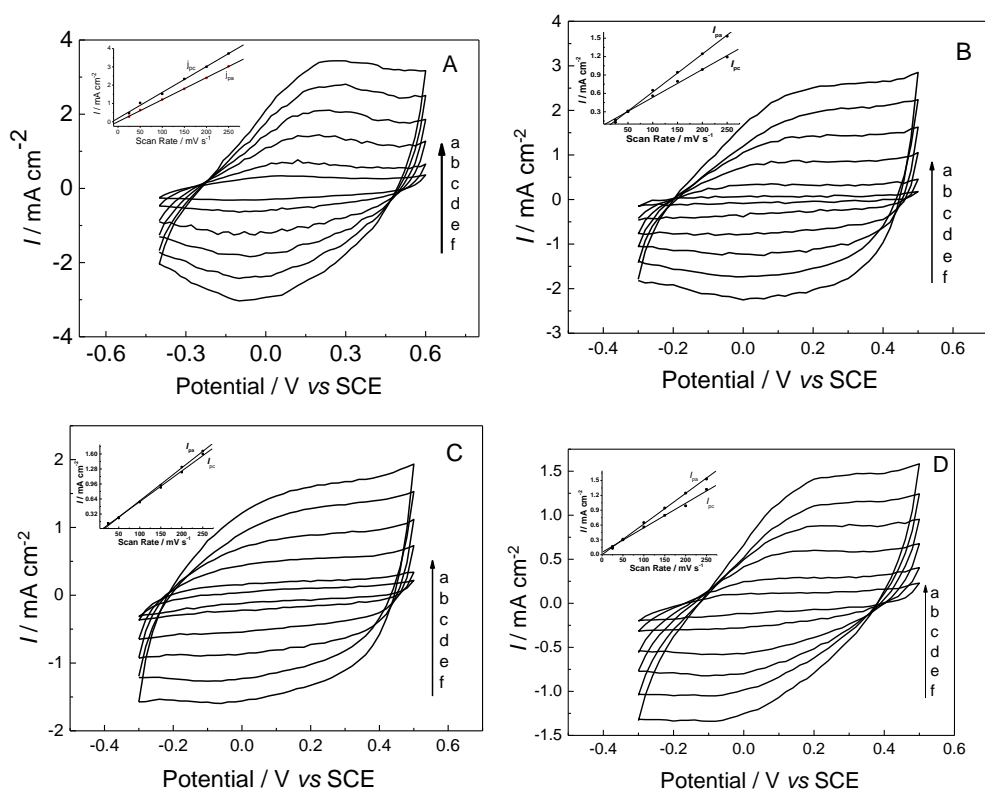


Figure 2. CVs of GCE/ILs-PEDOTM-MWCNTs-COOH in monomer-free electrolyte at potential scan rates of (a) 25 mV s⁻¹, (b) 50 mV s⁻¹, (c) 100 mV s⁻¹, (d) 150 mV s⁻¹, (e) 200 mV s⁻¹, and (f) 250 mV s⁻¹(A). The ILs-PEDOTM-MWCNTs-COOH was electro-synthesized in water/ILs mixed system containing BmimPF₆ with different mass ratios of EDOTM: MWCNTs-COOH = (B) 5:1, (C) 2:1, and (D) 1:2. Inset: graphs of redox peak current densities vs potential scan rates.

To evaluate the effect of MWCNTs-COOH on electrochemical properties of PEDOTM films, the electrochemistry of ILs-PEDOTM-MWCNTs-COOH composites was investigated by CVs in

monomer-free aqueous solutions (Fig. 2). All CVs (Fig. 2A–C) exhibited the broad oxidation and reduction peak, their current densities increased linearly with scanning rates in range $25\text{--}250\text{ mV s}^{-1}$ (Fig. 2 insert A–C), indicating that redox processes were not controlled by diffusion of counter-ions, reversible redox behaviors revealed that these ILs-PEDOTM-MWCNTs-COOH films were cycled repeatedly between the conducting and insulating states without significant decomposition. The broad anodic and cathodic peak suggested the obvious capacitance-like characteristic of PEDOT, which was also very similar to electrochemical characteristics of PEDOT in previous reports [27, 41]. The oxidation and reduction peak current densities in the insert of Fig. 2C were almost overlapping, which further indicated the best reversible redox behaviors of the ILs-PEDOTM-MWCNTs-COOH composites prepared in the mass ratio with 2:1 of EDOTM: MWCNTs-COOH.

3.2.2 Electrochemical stability of ILs-PEDOTM-MWCNTs-COOH

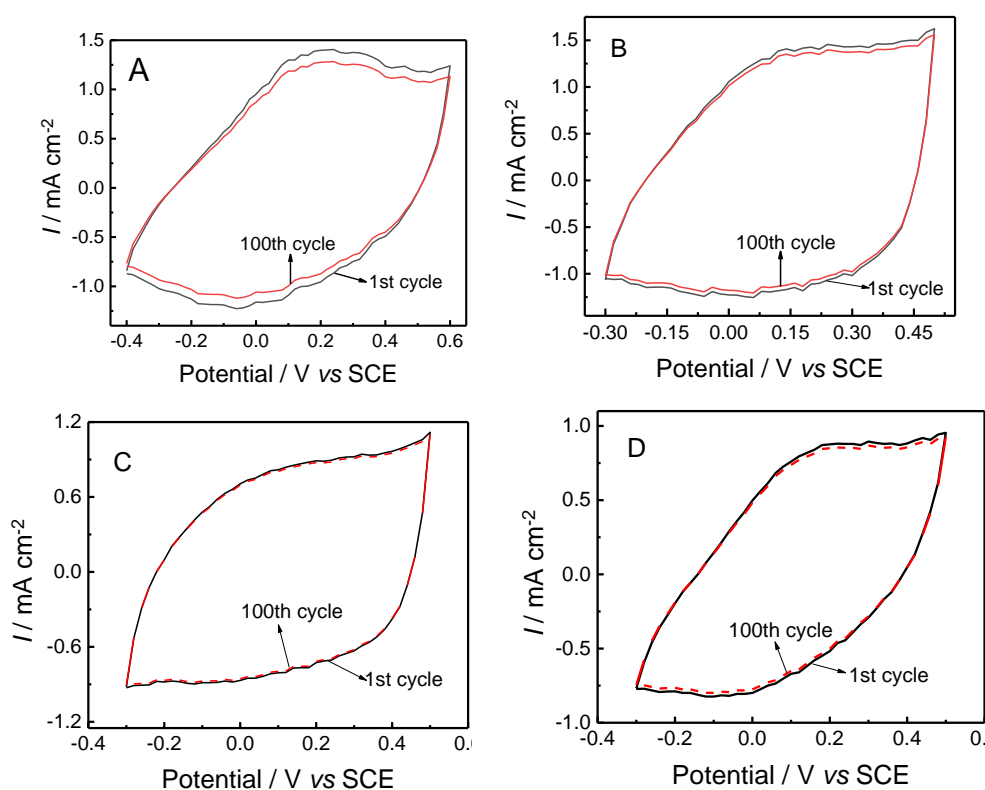


Figure 3. CVs of GCE/ILs-PEDOTM-MWCNTs-COOH in monomer-free electrolyte at potential scan rates of 50 mV s^{-1} (A). The ILs-PEDOTM-MWCNTs-COOH was electro-synthesized in water/ILs mixed system containing BmimPF₆ with different mass ratios of EDOTM: MWCNTs-COOH = (B) 5:1, (C) 2:1, and (D).

The CVs curves integral area ratios of the first cycle towards one hundredth cycle of the IL-PEDOTM was 8.7% (Fig. 3A), indicating there are no significant loss of their electroactivity ($<10\%$) when 100 redox cycles were carried out. While the CVs curves integral area ratios of the first cycle to one hundredth cycle of the ILs-PEDOTM-MWCNTs-COOH with mass ratios of 5:1, 2:1, and 1:2 was 4.9%, 1.5%, and 3% (Fig. 3B–D). revealing that three PEDOT films prepared in water/ILs mixed system containing BmimPF₆ were more stable, which were attributable to 3D network of MWCNTs-

COOH. All these results indicated that ILs-PEDOTM-MWCNTs-COOH film with mass ratios of 2:1 had best redox activity and highest stability.

All relative standard deviation (RSD) of redox peak currents of $[\text{Fe}(\text{CN})_6]^{3-/4-}$ for 100 times revealed that GCE/ILs-PEDOTM-MWCNTs-COOH had high stability due to no significant loss of electroactivity in an aqueous solution ($<2\%$), demonstrating that they were good stable and had good adhesive force between the ILs-PEDOTM-MWCNTs-COOH modified layer and the GCE surface (Fig. 4A), In addition, Ten GCE/ILs-PEDOTM-MWCNTs-COOH were fabricated independently for response current of $[\text{Fe}(\text{CN})_6]^{3-/4-}$, its RSD is 0.79% for oxidation peak and 0.76% for reduction peak (Fig. 4B), indicating excellent stability of GCE/ILs-PEDOTM-MWCNTs-COOH, which was used for the following experiments for immobilizing GOx.

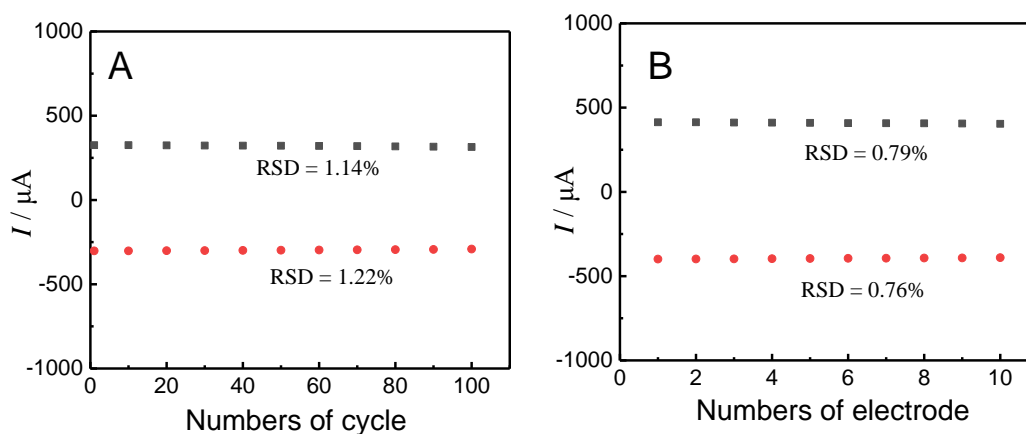


Figure 4. GCE/ILs-PEDOTM-MWCNTs-COOH were successively measured for 100 times by CVs using 5.0 mM $[\text{Fe}(\text{CN})_6]^{3-/4-}$ containing 0.1 M KCl (A). Ten GCE/ILs-PEDOTM-MWCNTs-COOH were measured by CVs using 5.0 mM $[\text{Fe}(\text{CN})_6]^{3-/4-}$ containing 0.1 M KCl (B).

3.3 Covalent immobilization of GOx

3.3.1 Electrochemical impedance spectroscopy

Fig. 5 demonstrated Nyquist plots of different electrodes with the real part (Z_{re}) on the x-axis and the imaginary part (Z_{im}) on the y-axis. The semicircle diameter in the impedance spectrum equates to the charge transfer resistance (R_{ct}) at the electrode surface. The increase or decrease in values of R_{ct} exactly characterized the modification of the electrode surface. The values of R_{ct} was 1960 Ω at the GCE/ILs-PEDOTM (Fig. 5A), The values of R_{ct} decreased (1230 Ω) when MWCNTs-COOH was doped into ILs-PEDOTM, indicating that MWCNTs-COOH in ILs-PEDOTM film enhanced the conductivity. The values of R_{ct} increased (3580 Ω) when GOx was covalently immobilized onto the surface of GCE/ILs-PEDOTM-MWCNTs-COOH, demonstrating that GOx was successfully immobilized onto the surface of GCE/ILs-PEDOTM-MWCNTs-COOH.

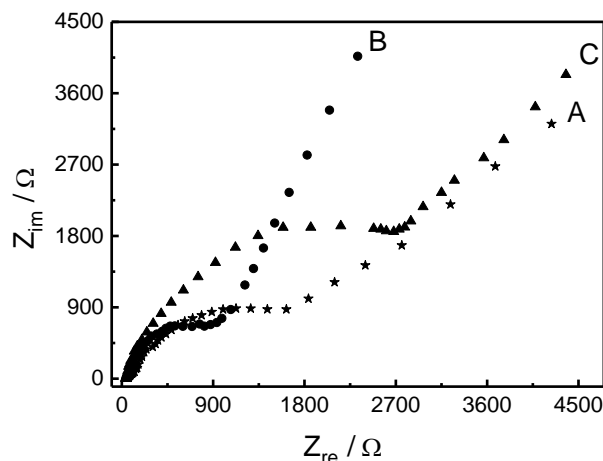


Figure 5. Nyquist plots of GCE/ILs-PEDOTM (A), GCE/ILs-PEDOTM-MWCNTs-COOH (B) and GCE/ILs-PEDOTM-MWCNTs-COOH/GOx (C) in the presence of 5 mM $[\text{Fe}(\text{CN})_6]^{3-/4-}$ containing 0.1 M KCl.

In addition, the apparent electrode coverage (θ) of the modified layer was calculated according to the equation as follows:

$$\theta = 1 - (R_b/R_m) \%$$

where R_b is the R_{ct} measured at a bare electrode, R_m is the R_{ct} measured at a modified electrode under same conditions [28,42,43]. The value of θ is about 65.64%, which also further confirmed that GOx were covalently immobilized onto the surface of ILs-PEDOTM-MWCNTs-COOH electrode.

3.3.2 Infrared spectroscopy

Fig. 6 shows FTIR spectra of different film. As can be seen from the FTIR spectrum of ILs-PEDOTM in Fig. 6A, the absorption band at 1639 cm^{-1} was assigned to the stretching vibration of the C=C and C=O bond in the thiophene ring, the band at 792 cm^{-1} were attributed to stretching vibration of C-S. The stretching modes of the ethylenedioxy group was at 1208 cm^{-1} , while the band around 983 cm^{-1} was due to the ethylenedioxy ring deformation mode. The band of 1105 cm^{-1} was assigned to the deformation vibration of C-H, while bands at 1369 and 1516 cm^{-1} were ascribed to the out-plane deformation vibration of C-H. In addition, the stretching vibration of O-H was 3218 cm^{-1} , all these are in accordance with previous reports [15]. In comparison with FTIR spectrum of ILs-PEDOTM, a strong absorption peak at 1639 cm^{-1} in Fig. 6B was likely to vibration of C-C due the presence of MWCNTs-COOH. In Fig. 6C, the absorption band at 1782 cm^{-1} are attributed to the stretching vibration of the C=O of GOx. Meanwhile, band at 3218 cm^{-1} disappeared. These indicated that GOx was covalently immobilized onto ILs-PEDOTM-MWCNTs-COOH matrix.

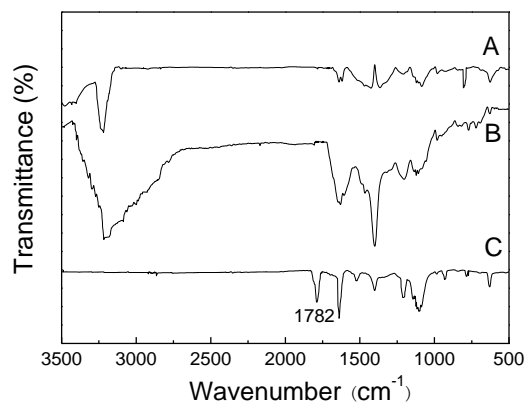


Figure 6. The FTIR spectra of ILs-PEDOTM (A), ILs-PEDOTM-MWCNTs-COOH (B), and ILs-PEDOTM-MWCNTs-COOH/GO_x (C).

3.4 Parametric optimization

3.4.1 Effect of working potential

Fig. 7A shows changes of response currents of the as-fabricated Glu biosensor based on ILs-PEDOTM-MWCNTs-COOH/GO_x at applied potentials ranging from 0 to 1.0 V. Response currents increased and reached a steady state value between 0 and 0.6 V, indicating that response currents were controlled by electrochemical processes and the kinetics of the enzyme-catalyzed reaction. But response currents became almost constant when applied potentials were more than 0.6 V, the relationship between response currents and applied potentials presented that response currents were largely independent of applied potentials in a range of 0.6 to 1.0 V (Fig. 7A). Therefore, 0.6 V was used as the optimal applied potential for the fabrication of Glu biosensor in following experiments.

3.4.2 Effect of PH

The relative enzyme activity increased from pH 5 to 8 and decreased when pH exceeded 7 (Fig. 7B), which was attributed to the acid and alkali towards the effect of GO_x. The response current of the Glu biosensor reached maximum at pH 7. Therefore, pH was optimum at pH 7, which employed in all experiments.

3.4.3 Effect of temperature

The effect of temperature between 10 and 50 °C on the relative bioactivity of the as-obtained biosensor was studied by current responses of the ILs-PEDOTM-MWCNTs-COOH/GO_x/GCE electrodes (Fig. 7C). The response currents gradually increased with the increasing temperature and reached a maximum 40 °C. The response current decreased sharply when the temperature exceeds 40 °C, which may be due to some enzyme inactivation caused by high temperature. The biosensor lost its bioactivity at temperatures above 40 °C, and eventually underwent the irreversible denaturation. The

very low temperature can influence the enzyme activity. The temperature has a smaller effect on the enzyme activity when the temperature exceeds 25 °C. To prevent irreversible gradual inactivation of GOx at higher temperatures at subsequent studies, 25 °C was selected for all following experiments.

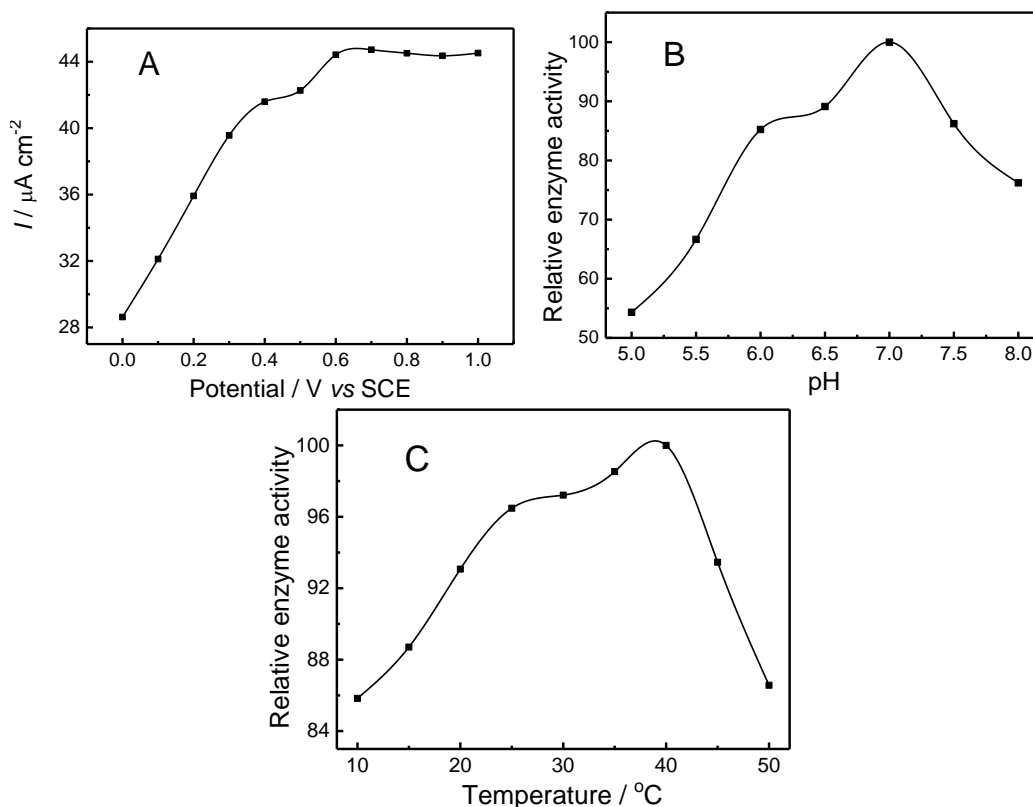


Figure 7. The effect of working potentials (A), pH (B), and temperature (C) of ILs-PEDOTM-MWCNTs-COOH/GOx biosensor.

3.5 Amperometric detection of Glu

Fig. 8 shows current responses of the fabricated GCE/IL-ILs-PEDOTM-MWCNTs-COOH/GOx biosensor towards Glu concentrations. The I value increased with the increase of [Glu] (Fig. 8), indicating that Glu was determined by the obtained GOx biosensor. In addition, $I-t$ curves of the biosensor displayed a fast response time (about 10 s). I vs [Glu] relationship indicated that there was a wide linearity of the response current versus [Glu] from $6.0 \times 10^{-8} \sim 2 \times 10^{-3}$ M ($R^2 = 0.994$) with a high sensitivity of $89.5 \mu\text{A M}^{-1} \text{cm}^{-2}$ (Fig. 8 inset), LOD is $0.015 \mu\text{M}$ ($S/N = 3$). All these indicated that this is suitable for measuring Glu with unknown content.

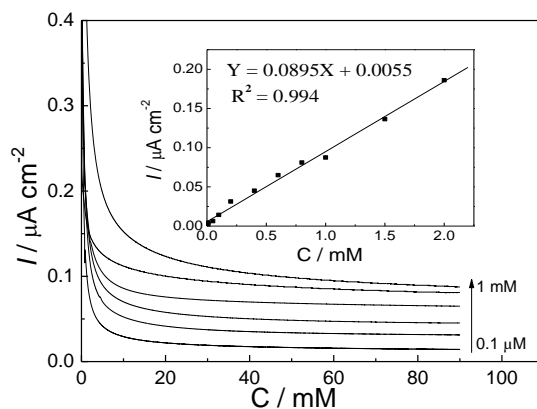


Figure 8. The $I-t$ curves of response current with the Glu concentration on ILs-PEDOTM-MWCNTs-COOH/GOx biosensor for the detection of Glu at the working potential of 0.6 V. Inset: Calibration plots for response currents of ILs-PEDOTM-MWCNTs-COOH/GOx biosensor vs different Glu concentrations.

A comparison analysis on amperometric detection of Glu using different electrode modified electrodes reported in the literature was listed in Table 1. It could be seen that ILs-PEDOTM-MWCNTs-COOH offered wide linear range and low LOD for the detection of Glu. This result indicated that ILs modified high conducting and biocompatible PEDOTM-MWCNTs nanocomposite is an excellent biosensing matrix for the development of electrochemical biosensing platform.

Table 1 Comparison of the sensing performance of GOx biosensor based on different electrodes for the Glu amperometric analysis.

Electrodes	Linear range (M)	LOD (μM)	Reference
AuNPs/G/MWCNTs		4.8	[44]
graphene/PANI/AuNPs	$4 \times 10^{-6} - 1.12 \times 10^{-3}$	0.6	[45]
RGO/Ag	$0.5 \times 10^{-3} - 12.5 \times 10^{-3}$	160	[46]
MoS ₂ /AuNPs	$0.1 \times 10^{-5} - 3 \times 10^{-4}$	2.8	[47]
Au-ZnO	$4 \times 10^{-3} - 2 \times 10^{-2}$	20	[48]
Fe ₃ O ₄ @Au	$2 \times 10^{-4} - 9 \times 10^{-3}$	100	[49]
Pistol-like DNAzyme	$1.0 \times 10^{-11} - 1 \times 10^{-2}$	5	[50]
IL-ILs-PEDOTM-MWCNTs-COOH	$6.0 \times 10^{-8} - 2 \times 10^{-3}$	0.0033	work

3.6 Biosensing performance

3.6.1 Bioaffinity and biocompatibility

Fig. 9A presents the relationship between steady-state currents of the fabricated Glu biosensor based on GCE/IL-ILs-PEDOTM-MWCNTs-COOH/GOx and Glu concentrations, Response currents increased with increasing glucose concentrations, indicating that Glu was determined using the as-developed GOx biosensor. The response currents of GCE/ILs-PEDOTM-MWCNTs-COOH/GOx

tended almost to be constant when the glucose concentration exceeded 2×10^{-3} M, which was assigned to the saturation of GOx with the increase of glucose concentrations.

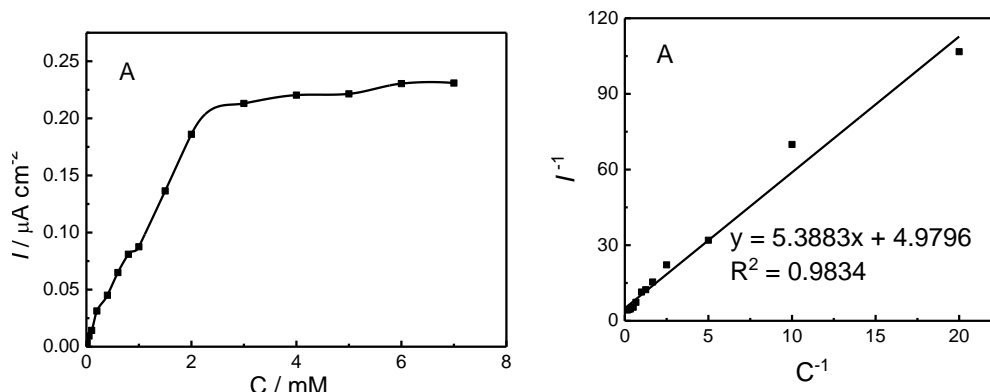


Figure 9. The relationship between response currents of the fabricated Glu biosensor and Glu concentrations (A). Lineweaver-Burk plots of Glu biosensor based on ILs-PEDOTM-MWCNTs-COOH/GOx under optimal conditions (B).

The bioaffinity of the as-obtained electrochemical Glu biosensor was obtained by describing the relationship between steady-state response currents and Glu concentrations, which was given by Lineweaver–Burk plots (Fig. 9B). The apparent Michaelis–Menten constant (K_m) was obtained by the Lineweaver–Burk equation as follows:

$$1/I = 1/I_{\text{max}} + K_m / I_{\text{max}} C$$

where I is the steady-state response current, C represents the concentration of Glu, s and I_{max} is the maximum steady-state apparent response current. After linear regression, The I_{max} was 0.2 mA cm^{-2} , K_m was 1.08 mM , The Michaelis–Menten constant is inversely proportional to enzymatic affinity for its substrates [51-54], which significantly less than the K_m value of natural GOx, indicating that more substrates were associated with GOx in the PEDOTM-MWCNTs-COOH matrix of the as-obtained electrochemical Glu biosensor.

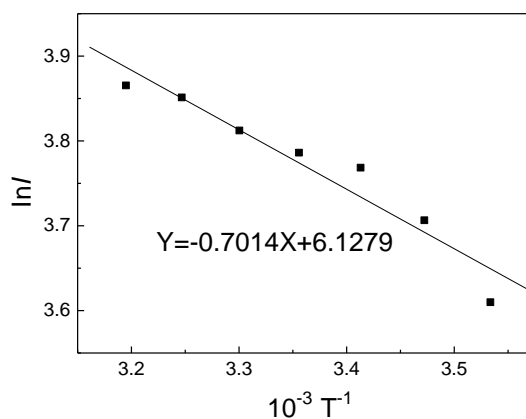


Figure 10. The graph of the $\ln I$ vs T^{-1} for ILs-PEDOTM-MWCNTs-COOH/GOx biosensor.

The apparent activation energy (E_a) of the as-obtained GOx biosensor was plotted by $\ln I$ vs. $1/T$ graphs (Fig. 10), which depicted the relationship between the Napierian logarithm of I and the inverse of the temperature. The E_a was obtained by the equation as follows:

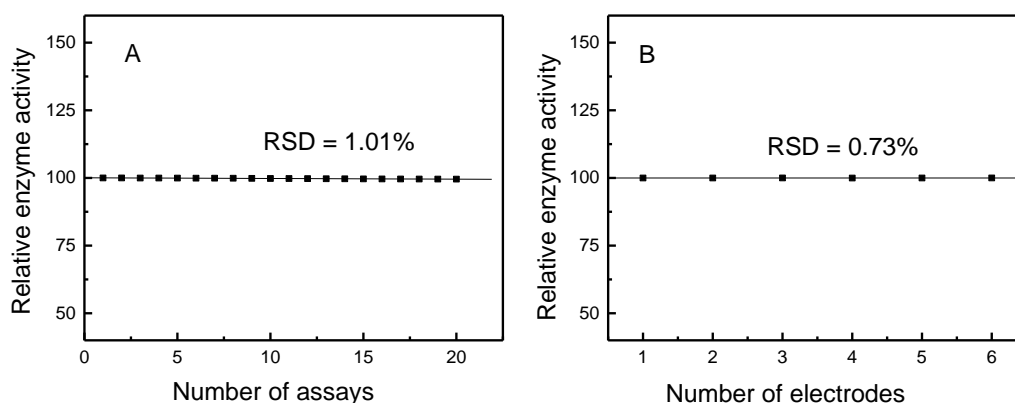
$$\ln I = \ln I_0 + E_a / RT$$

Here, I stand for the steady-state response current, I_0 is a collection of currents, R and T have their usual meanings. After linear regression, the E_a for the enzymatic reaction in the ILs-PEDOTM-MWCNTs-COOH matrix of the as-obtained Glu biosensor was 5.83 kJ M^{-1} . A low E_a implied that good bioactivity and affinity for its substrates (Glu) of GOx that was covalently immobilized into the ILs-PEDOTM-MWCNTs-COOH matrix of the biosensor, which was in accordance with the low K_m . The low E_a and K_m also further indicated that the electrochemically synthesized PEDOTM-MWCNTs-COOH matrix had good biocompatibility and affinity.

3.6.2 Stability

The repeatability of the fabricated GOx biosensor based on GCE/ILs-PEDOTM-MWCNTs-COOH matrix for the amperometric detection of 2 mM Glu was estimated by 20th successive assays (Fig. 11A), and its RSD value was 1.01%, indicating an acceptable repeatability of the fabricated GOx biosensor. Afterwards, six GCE/ILs-PEDOTM-MWCNTs-COOH/GOx were used for the reproducibility of the sensing electrode (Fig. 11B), and its RSD of 0.73% was obtained, indicating the good reproducibility of the fabricated GOx biosensor.

To evaluate the lifetime (storage stability) of the as-fabricated GOx biosensor, each measurement was implemented periodically every day in PBS at $4 \text{ }^\circ\text{C}$ for 30 days (Fig. 11C). Moreover, each measurement was repeated three times, and each data point stands for the average values of triplicate tests. No loss of the relative enzyme activity was observed for one week, and the relative enzyme activity decreased approximately 0.9% after being stored for 15 days. Besides, 98.3% of bioactivity still retained after the biosensor was stored for 30 days. In addition, RSD values of 30 days for 30 assays is 0.54%. All results indicated that the as-obtained biosensor based on GCE/ILs-PEDOTM-MWCNTs-COOH/GOx.



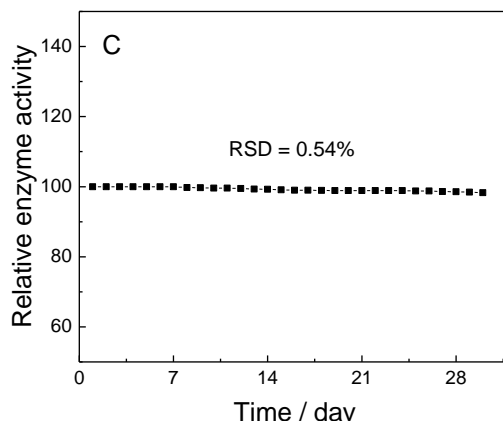


Figure 11. The repeatability (A), reproducibility (B), and storage stability (C) of the as-fabricated Glu biosensor based on GCE/ILs-PEDOTM-MWCNTs-COOH/GOx.

3.6.3 Practicality

Table 2 lists the detection of Glu content in different biological samples, which were acquired by the as-fabricated GOx biosensor based on GCE/ILs-PEDOTM-MWCNTs-COOH matrix using the standard addition method in comparison with HPLC method. The obtained results using HPLC method are in better accordance with that of the as-fabricated GOx biosensor, indicating that the biosensing method is feasible and suitable. Besides, the known amounts of Glu were added into different samples, then were measured. The recovery values of all samples are in a range of 96.8% – 101.2%, indicating that the obtained Glu biosensor based on GCE/ILs-PEDOTM-MWCNTs-COOH/GOx was used for the detection of Glu in practical samples. RSD values for the analysis of all practical samples were less than 3%, revealing that the accuracy of the fabricated biosensor was acceptable in animal and human urines and serums.

Table 2. The measurement of Glu in practical samples using GOx electrochemical biosensor in comparison with HPLC method.

Samples	biosensing method				HPLC method		
	Added (μM)	found (μM)	RSD (%)	Recovery (%)	Found (μM)	RSD (%)	Recovery (%)
Human urine	0	3.23 ± 0.08	2.5		2.67 ± 0.03	1.1	
	20	23.64 ± 0.29	1.2	101.8	22.8 ± 0.35	1.5	100.6
Human serum	0	36.27 ± 0.54	1.5		34.7 ± 0.51	1.4	
	20	55.64 ± 0.98	1.8	99.9	55.37 ± 0.86	1.6	101.2
Bovine serum	0	22.83 ± 0.37	1.6		24.3 ± 0.43	1.8	
	20	43.43 ± 0.96	2.2	101.4	43.54 ± 0.69	1.6	98.3
Pig serum	0	20.48 ± 0.37	1.8		18.8 ± 0.23	1.2	
	20	39.36 ± 0.58	1.5	97.2	37.56 ± 0.43	1.2	96.8

4. CONCLUSIONS

An electrochemical Glu biosensor based on GCE/ILs-PEDOTM-MWCNTs-COOH/GOx was successfully fabricated for the amperometric detection of Glu in human urine, human and animal serum samples. A highly-stable and conducting PEDOTM film was one-step electro-synthesized in water/ILs mixed system containing BmimPF₆ and MWCNTs-COOH. GOx was covalently immobilized onto the biocompatible and conducting ILs-PEDOTM-MWCNTs-COOH matrix. CVs and EIS confirmed that ILs-PEDOTM-MWCNTs-COOH displayed excellent electrochemical stability, high conductivity and good covalent immobilization of GOx. The as-fabricated Glu biosensor based on GCE/ILs-PEDOTM-MWCNTs-COOH/GOx displayed high amperometric response current toward Glu in a linear range of $6.0 \times 10^{-8} \sim 2 \times 10^{-3}$ M with a high sensitivity of $89.5 \mu\text{A M}^{-1} \text{cm}^{-2}$, fast response time within 10 s, low LOD (0.015 μM), remarkable biocompatibility, high sensing stability, excellent bioaffinity, high selectivity and satisfactory practicality.

ACKNOWLEDGEMENTS

The authors would like to appreciate of financial support from NSFC (31460540) and Jiangxi Provincial Department of Education (GJJ160412).

References

1. J. Wang, *Electroanal.*, 13 (2001) 983.
2. E. H. Yoo and S.Y. Lee, *Sensors*, 10 (2010) 4558.
3. J. D. Newman, *Biosens. Bioelectron.*, 20 (2005): 2435.
4. C. Chen, Q.J. Xie, D.W. Yang, H.L. Xiao, Y.C. Fu, Y.M. Tan and SZ. Yao, *RSC Adv.*, 3 (2013) 4473.
5. J. Wang, *Chem. Rev.*, 108 (2008) 814.
6. M. Singh, P. K. Kathuroju and N. Jampana, *Sens. Actuat. B.*, 143 (2009) 430.
7. Z.G. Zhu, L. Garcia-Gancedo, A.J. Flewitt, H.Q. Xie, F. Moussy and W.I. Milne, *Sensors*, 12 (2012) 5996.
8. M.M. Rahman, A.J. Ahammad, J.H. Jin, S.J. Ahn and J.J. Lee, *Sensors*, 10 (2010) 4855.
9. L. Groenendaal, F. Jonas, D. Freitag, H. Pielartzik and J. R. Reynolds *Adv. Mater.*, 12 (2000) 481.
10. S. Kirchmeyer and K. Reuter, *J. Mater. Chem.*, 15 (2005) 2077.
11. Y.P. Wen and J.K. Xu, *J. Polym. Sci. A: Polym. Chem.*, 55 (2017) 1121.
12. Y. Hui, C. Bian, S. Xia, J. Tong, J. Wang, *Anal. Chim. Acta*, (2018), In Press
13. L. Groenendaal, G. Zotti, P.H. Aubert and S.M. Waybright, *Adv. Mater.*, 2003, 15 (3003) 879.
14. N. Rozlosnik. *Anal. Bioanal Chem.*, 395 (2009) 637.
15. Y.P. Wen, D. Li, Y. Lu, H.H. He, J.K. Xu, X.M. Duan and M. Liu, *Chinese J. Polym. Sci.*, 30 (2013) 460.
16. Y. Lu, Y.P. Wen, B.Y. Lu, X.M. Duan, J.K. Xu, L. Zhang and Y. Huang, *Chinese J. Polym. Sci.*, 30(2012) 824.
17. Y. Xiao, X. Cui, J.M. Hancock, M. Bouguettaya, J.R. Reynolds and D.C. Martin, *Sens. Actuat. B.*, 99 (2004) 437.
18. Z.L. Feng, Y.Y. Yao, J.K. Xu, L. Zhang, Z.F. Wang and Y.P. Wen, *Chinese Chem. Lett.*, 25(2014) 511.
19. Zhao H, *J. Chem. Technol. Biotechnol.*, 85 (2010) 891.
20. D.S. Silvester, *Analyst*, 136 (2001) 4871.

21. M.J.A. Shiddiky and A.A.J. Torriero. *Biosens. Bioelectron.*, 26(2011) 1775.
22. D. Wei and A. Ivaska, *Anal. Chim. Acta*, 2008, 607(2): 126-135.
23. F. Khaleghi, A.E. Irai, R. Sadeghi, V.K. Gupta and Y.P. Wen, *Sensors*, 16 (2016) 747.
24. H. Mazurkiewicz, P.C. Innis, G.G. Wallace, D.R. MacFarlane and M. Forsyth, *Synth Met*, 135 (2003) 31.
25. B. Dong, J.K. Xu and L.Q. Zheng, *Prog. Chem.*, 21 (2009) 1792.
26. J. Lu, F. Yan and J. Texter, *Prog. Polym. Sci.*, 34 (2009) 431.
27. D. Li, Y.P. Wen, J.K. Xu, H.H. He and M Liu. *Chinese J. Poly. Sci.*, 30 (2012) 705.
28. Y.P. Wen, X.M. Duan, J.K. Xu, R.R. Yue, D. Li, M. Liu and L. Lu, *J. Solid State Electrochem.*, 16 (2012) 3725.
29. Y.P. Wen, D. Li, J.K. Xu, X.Q. Wang and H.H. He. *Int. J. Polym. Mater. Po.*, 62 (2013) 437.
30. C.B. Jacobs, M.J. Peairs and B.J. Venton, *Anal. Chim. Acta*, 662 (2010) 105.
31. C. Gao, Z. Guo, J.H. Liu and X.J. Huang. *Nanoscale*, 4 (2012) 1948.
32. J. Wang. *Electroanal.*, 2005, 17 (2005) 7.
33. J.J. Gooding, *Electrochim. Acta*, 50 (2005) 3049.
34. M Trojanowicz, *TrAC trend. Anal. Chem.*, 25(2006) 480.
35. Y.Q. Peng, W.J. Zhang, J Chang, Y.P. Huang, Chen, H. Deng. Z. Huang and Y.P. Wen, *Food Anal. Method.*, 10 (2017) 3375.
36. Y.Y. Yao, L Zhang, J.K. Xu, X.Q. Wang, X.M. Duan and Y.P. Wen, *J. Electroanal. Chem.*, 713 (2014) 1-8.
37. L. Zhang, Y.P. Wen, Y.Y. Yao, Z.F. Wang, X.M. Duan and J.K. Xu, *Chinese Chem. Lett.*, 25 (2014) 517.
38. Y.Y. Yao, X.M. Zhang, N. Li, X.M. Liang, Y.P. Wen, H. Zhang, Y.L. Chen, D.J. Yang and J.K Xu, *Int. J. Electrochem. Sci.*, 11 (2016) 5427.
39. G.B. Liu, C.X. Deng, X.N. Liao, XQ. Wang, M.F. Li, Y.D. Lan, Y.Q. Peng and Y.P. Wen, *Int. J. Electrochem. Sci.*, 11 (2016) 650.
40. M. Liu, Y.P. Wen, J.K. Xu, H.H. He, D. Li, R.R. Yue and G.D. Liu, *Anal. Sci.*, 27 (2010) 477.
41. M. Liu, Y.P. Wen, D. Li, R.R. Yue, J.K. Xu and H.H. He, *Sens. Actuat. B.*, 159 (2011) 277.
42. M. Liu, Y.P. Wen, D. Li, H.H. He, J.K. Xu, C.C. Liu, R.R. Yue, B.Y. Lu and G.D. Liu, *J. Appl. Polym. Sci.*, 122 (2011) 1142.
43. E. Sabatani, J. Cohen-Boulakia, M. Bruening and I. Rubinstein, *Langmuir*, 9 (1993) 2974.
44. Y. Yu, Z.G. Chen, S. He, B. Zhang, X. Li and M. Yao, *Biosen. Bioelectron.*, 2 (2014) 147.
45. Q. Xu, S.X. Gu, L. Jin, Y. Zhou, Z. Yang, W. Wang and X. Hu, *Sens. Actuat. B.*, 190(2004) 562.
46. S. Palanisamy, C. Karuppiah and S.M. Chen, *Colloid. Surface. B.*, 114(2014) 164.
47. S. Su, H. Sun, F. Xu, L. Yu, C. Fan and L. Wang, *Microchim. Acta*, 181(2014) 1497.
48. A. Samphao, P. Butmee, J. Jitcharoen, L. Švorc, G. Raber and K. Kalcher, *Talanta*, 181(2014) 1497.
49. C. Wu, H. Sun, Y. Li, X. Liu, X. Du, X. Wang and P. Xu, *Biosen. Bioelectron.*, 66 (2015) 350.
50. C. Liu, Y. Sheng, Y. Sun, J. Feng, S. Wang, J. Zhang, J. Xu and D. Jiang, *Biosen. Bioelectron.*, 70 (2015) 455.
51. D. Li, Y.P. Wen, H.H. He, J.K. Xu, M. Liu and R.R. Yue, *J. Appl. Polym. Sci.*, 126 (2012) 882.
52. A.G. Marangoni, *Enzyme Kinetics: A Modern Approach*, John Wiley and Sons, Inc., USA, 2003.
53. Y.P. Wen, J.K. Xu, M Liu, D Li, L.M. Lu, R.R. Yue and H.H. He, *J. Electroanal. Chem.*, 674 (2012) 71.
54. J.Y. Wang, S.G. Zhu and C.F. Xu, *Biochemistry*, Higher Education Press, Beijing, 2002.